

# Melting experiments of a chondritic meteorite between 16 and 25 GPa: Implication for Na/K fractionation in a primitive chondritic Earth's mantle

MING CHEN<sup>1,2,\*</sup>, AHMED EL GORESY<sup>2</sup>, DAN FROST<sup>3</sup> and PHILIPPE GILLET<sup>4</sup>

<sup>1</sup>Guangzhou Institute of Geochemistry, Chinese Academy of Sciences, 510640 Guangzhou, P.R. China.

\*Corresponding author, e-mail: mchen@gig.ac.cn

<sup>2</sup>Max-Planck-Institut für Chemie, D-55128 Mainz, Germany

<sup>3</sup>Bayerisches Geoinstitut, Universität Bayreuth, D-95440 Bayreuth, Germany

<sup>4</sup>Ecole Normale Supérieure de Lyon, F-69364 Lyon Cedex, France

**Abstract:** Melting experiments at high-pressure and temperature were conducted at pressures from 16 to 25 GPa using chondritic starting material but with slightly enhanced Na- and K-contents while keeping the chondritic Na/K ratio constant. The experiments revealed that majorite garnet contains enhanced concentrations of Na (3.75–4.71 wt.% Na<sub>2</sub>O) and moderately enhanced concentrations of K (0.3–0.46 wt.% K<sub>2</sub>O) from 16 to 20 GPa and it is therefore the Na- and K-bearing phase at this pressure range. The Na<sub>2</sub>O/K<sub>2</sub>O ratio (8–15) in garnet is close to the initial chondritic ratio (7) of the starting material, which might indicate that at these pressures only little Na/K fractionation takes place. At pressures above 21 GPa, the high-pressure phases enriched in Na include majorite garnet (3.08–6.22 wt.% Na<sub>2</sub>O), magnesiowüstite (1.83–3.3 wt.% Na<sub>2</sub>O), and (Mg,Fe)SiO<sub>3</sub>-perovskite (0.43–1.25 wt.% Na<sub>2</sub>O). These phases contain only small amounts of K (<0.1 wt.% K<sub>2</sub>O). The Na<sub>2</sub>O content of magnesiowüstite progressively increases with increase of pressure, whereas Na<sub>2</sub>O contents of garnet and perovskite are negatively correlated with pressures between 23 and 25 GPa. Na/K fractionation takes place among the high-pressure phases (Na<sub>2</sub>O/K<sub>2</sub>O ratio: 56–102 in garnet, 5–20 in perovskite, and 43–94 in magnesiowüstite), and between the high-pressure phases and the residual silicate melt above 21 GPa, and most of the K is partitioned into the residual melt. The hollandite-structured, high-pressure KAlSi<sub>3</sub>O<sub>8</sub> polymorph crystallizes from the liquid at 23 GPa. These results demonstrate that Na/K fractionation at P > 21 GPa should have taken place in the early accretional period in the primitive chondritic mantle of the Earth.

**Key-words:** melting experiment, high pressure, chondritic meteorite, alkali element, fractionation.

## 1. Introduction

Na and K are important alkali elements in chondritic meteorites. Carbonaceous chondrites contain 0.42–0.83 wt.% Na<sub>2</sub>O and 0.03–0.08 wt.% K<sub>2</sub>O, and ordinary chondrites contain 0.78–1.06 wt.% Na<sub>2</sub>O and 0.07–0.11 wt.% K<sub>2</sub>O (Kallemeyn, 1988). The Na<sub>2</sub>O/K<sub>2</sub>O ratio (7–10) in these chondritic meteorites is generally accepted to be the solar ratio. The Earth is believed to have formed through the accretion of planetesimals composed of silicates and metals (Mason, 1966; Ringwood, 1975; Morgan *et al.*, 1980). Because ordinary chondrites are the most abundant terrestrial meteorite falls, chondritic planetesimals could have been a major source feeding the accreting Earth in the earliest evolutionary stage. Therefore, experiments conducted on chondritic meteorites could give a close insight into the early evolution of the Earth's primitive chondritic mantle.

Both Na and K are lithophile in ordinary chondrites, and are usually incorporated in plagioclase feldspar with oligoclase to andesine composition. The hollandite-structured high-pressure polymorphs of feldspars NaAlSi<sub>3</sub>O<sub>8</sub> and KAl-

Si<sub>3</sub>O<sub>8</sub>, were reported in shock-melt veins in L-chondrites and in an SNC meteorite (Gillet *et al.*, 2000; Chen & El Goresy, 2000; El Goresy *et al.*, 2000; Langenhorst & Poirier, 2000). The NaAlSi<sub>3</sub>O<sub>8</sub> end-member is stable at high pressures below 23 GPa (Liu, 1978; Yagi *et al.*, 1994).

The melting experiments on anhydrous peridotite at pressures from 5–22.5 GPa (Herzberg & Zhang, 1996) and carbonaceous meteorite at pressures up to 27 GPa (Agee *et al.*, 1995) indicated that the majorite/liquid and magnesiowüstite/liquid partition coefficients for Na increase with increase of pressure. High-pressure experiments on pyrolite at 28 GPa also revealed that Na partitions more favorably into magnesiowüstite than into coexisting MgSiO<sub>3</sub>- or CaSiO<sub>3</sub>-perovskites (Irifune, 1994). Neither (Mg,Fe)SiO<sub>3</sub>-perovskite, magnesiowüstite, ringwoodite, wadsleyite, nor ilmenite has sites large enough to accommodate the large K cation. Recent subsolidus and melting experiments on K-rich basalt revealed that K-hollandite appears above the solidus at pressures above 22.5 GPa, and that majorite garnet may contain significant amounts of K at higher pressures between 25 and 27 GPa (Wang & Takahashi, 1999). Howev-

Table 1. Compositions of starting material (M' bale L-chondrite) in wt.%.

	Original		Modified	
	Bulk	Oxides*	Bulk	Oxides*
SiO <sub>2</sub>	42.18	48.04	46.30	51.95
Al <sub>2</sub> O <sub>3</sub>	1.99	2.27	2.22	2.49
TiO <sub>2</sub>	0.12	0.14	0.10	0.11
Cr <sub>2</sub> O <sub>3</sub>	0.51	0.58	0.45	0.50
FeO	15.95	18.16	14.10	15.82
MnO	0.10	0.11	0.09	0.10
MgO	23.58	26.85	20.85	23.41
CaO	2.42	2.76	2.14	2.40
Na <sub>2</sub> O	0.84	0.95	2.50	2.80
K <sub>2</sub> O	0.12	0.14	0.36	0.40
P <sub>2</sub> O <sub>5</sub>	0.26		0.23	
Fe	5.65		4.91	
Ni	0.89		0.79	
Co	0.23		0.20	
Cu	0.01		0.01	
FeS	5.24		4.64	
Totals	99.88	100	99.90	100
Mg#		0.73		0.73
Na <sub>2</sub> O/K <sub>2</sub> O	7	7	7	7

Oxides\* are normalized to 100%. Mg# = MgO/(MgO+FeO)

er, further experiments on K-doped peridotite between 10 and 27 GPa (Wang & Takahashi, 2000) revealed that garnet was not the main K-bearing phase and that K-hollandite was also not present.

We have previously investigated Na/K fractionation among dense phases occurring in the shock-melt veins of naturally shocked L-chondrites, where phase assemblages seemed to be comparable to the phase mineralogy in the transition zone and lower mantle of the Earth. Our studies of natural high-pressure assemblages in the shock-melt veins of Sixiangkou, Tenham, Peace River and M' bale L6-chondrites indicated the presence of the high-pressure assemblage of majorite-pyrop solid solution plus magnesiowüstite and that the majoritic garnet acquired most of the Na (0.99 wt.%) from the shock-produced chondritic melt (1.13 wt.% in bulk), whereas a K-bearing mineral was not identified (Chen *et al.*, 1996; El Goresy *et al.*, 1997a, 1997b). We envisage that K/Na fractionation in the Earth's primitive chondritic mantle might have taken place among high-pressure phases, or between high-pressure phases and residual melt. In this study, we conducted high-pressure and temperature experiments on an L6-chondrite at pressures from 16 to 25 GPa in order to explore the K and Na partitioning behaviour among high-pressure phases and between high-pressure phases and melt.

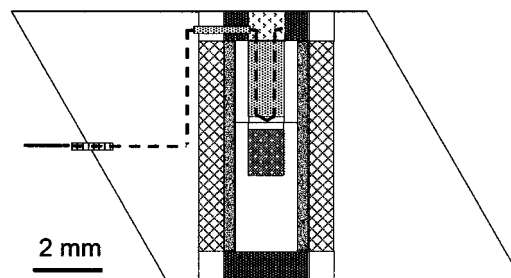
## 2. Experimental methods

The starting material used in this study was powdered M' bale (L6) chondrite. In order to allow Na and K to be analyzed with confidence in the run products by electron microprobe, additional Na<sub>2</sub>Si<sub>2</sub>O<sub>5</sub> and KAlSi<sub>3</sub>O<sub>8</sub> glasses were added to the starting material. The Na<sub>2</sub>O and K<sub>2</sub>O concen-

Table 2. Inventory of multi-anvil experiments.

Run no.	Pressure (GPa)	Temperature (°C)	High-pressure assemblage	Content of melt glass (vol.%)
H 2366	25	2000	Pv, Gt, Mw	<0.5
H 2237	24	2100	Gt, Pv, Mw	~2
H 2236	23	2000	Gt, Pv, Mw, Hlt	~2
H 2368	21	2000	Gt, Mw	<0.5
H 2547	20	1950	Gt, Rgt	<0.5
H 2549	18	1900	Gt, Rgt	<0.5
H 2548	16	1900	Gt, Rgt, Wds	<0.5

Pv: (Mg,Fe)SiO<sub>3</sub> perovskite; Gt: majorite garnet; Rgt: ringwoodite; Wds: wadsleyite; Hlt: KAlSi<sub>3</sub>O<sub>8</sub>-hollandite; Mw: magnesiowüstite.



Legend: MgO (white), Al<sub>2</sub>O<sub>3</sub> (diagonal lines), Sample (hatched), Mo (cross-hatched), Cu coil (vertical lines), ZrO (diagonal lines), LaCrO<sub>3</sub> (cross-hatched), Pyrophyllite (dotted), W/Re thermocouple (dashed line).

Fig. 1. A sketch of cross section of octahedron in the 10/4 multi-anvil assemblies.

trations were increased by 3 times the original chondrite's content, such that the Na<sub>2</sub>O/K<sub>2</sub>O ratio was kept in a chondritic ratio (Na<sub>2</sub>O/K<sub>2</sub>O = 7). The Mg# (a Mg-value, Mg# = MgO/(MgO+FeO)) of the starting material with added Na<sub>2</sub>Si<sub>2</sub>O<sub>5</sub> and KAlSi<sub>3</sub>O<sub>8</sub> glass was 0.73, which is identical to that of the original chondrite (Table 1). The compositional differences between the starting material and the original chondrite are minor and should have no influence on melting temperature and crystallization path. The sample was crushed using an agate mortar and pestle, ground and thoroughly mixed to a fine homogeneous powder.

High-pressure experiments were performed in the pressure range 16 to 25 GPa and temperatures between 1900 and 2100 °C in the Sumitomo UHP 1200 multi-anvil device at the Bayerische Geoinstitut, Universität Bayreuth, Germany. The 10-mm edge length MgO octahedra were employed with 4-mm edge length WC cube truncations. LaCrO<sub>3</sub> heaters and MgO sample capsules were used in the assembly (Fig. 1). Temperature was monitored by WRe<sub>3</sub>/WRe<sub>25</sub> thermocouples. All experiments were brought to the desired run pressure at room temperature, and then subsequently brought to complete melting by heating above the melting temperature for 5 minutes. Our previous investigation showed that an equilibrium phase assemblage of majorite plus magnesiowüstite was produced in the shock-melt veins of chondritic meteorites in a short duration of presumably few seconds in impact events (Chen *et al.*, 1996). The time duration of 5 minutes of complete melting of the experi-

Table 3. Compositions of experimentally produced high-pressure phases in wt.%.

	H 2366				H 2237				H 2236					H 2368		H 2547				H 2549				H 2548										
	Gt	S.D.	Pv	S.D.	Gt	S.D.	Pv	S.D.	Gt	S.D.	Pv	S.D.	Hlt	S.D.	Gt	S.D.	Gt	S.D.	Rgt	S.D.	Gt	S.D.	Rgt	S.D.	Gt	S.D.	Rgt	S.D.	Gt	S.D.	Rgt	S.D.	Wds	S.D.
	(10)		(10)		(10)		(5)		(10)		(5)		(5)		(10)		(10)		(5)		(10)		(5)		(10)		(5)		(10)		(5)		(5)	
SiO <sub>2</sub>	55.65	1.76	55.79	0.40	56.66	2.66	56.80	0.80	57.69	1.44	56.7	0.32	66.00	0.65	54.28	0.90	55.84	0.22	40.39	0.11	53.94	0.39	40.18	0.48	53.91	0.20	39.99	0.13	41.08	0.08				
Na <sub>2</sub> O	4.11	1.46	0.43	0.15	5.57	0.76	0.79	0.32	6.22	0.44	1.25	0.68	0.80	0.12	3.08	0.52	3.75	0.47	0.42	0.12	3.86	0.72	0.61	0.07	4.71	0.15	0.69	0.09	0.68	0.05				
K <sub>2</sub> O	0.05	0.02	0.09	0.03	0.07	0.06	0.04	0.04	0.11	0.07	0.10	0.05	15.62	0.38	0.03	0.01	0.46	0.12	0.14	0.15	0.35	0.02	0.06	0.05	0.30	0.14	0.01	0.05	0.13	0.02				
TiO <sub>2</sub>	0.02	0.03	0.14	0.05	0.04	0.02	0.18	0.05	0.06	0.02	0.18	0.11	0.00	0.01	0.01	0.04	0.07	0.04	0.01	0.02	0.13	0.03	0.00	0.00	0.13	0.03	0.00	0.02	0.00	0.00				
FeO	5.66	0.87	5.88	1.11	6.22	0.37	8.44	1.78	7.15	0.45	8.18	0.41	0.78	0.02	7.80	0.43	6.88	0.72	16.15	0.70	7.88	0.63	14.90	1.43	6.85	0.29	19.28	0.93	12.99	0.75				
Al <sub>2</sub> O <sub>3</sub>	9.08	0.92	1.71	0.66	8.35	3.18	0.42	0.18	8.68	2.84	0.31	0.09	17.64	0.59	7.59	2.19	7.30	1.17	0.42	0.08	7.98	0.71	0.39	0.09	9.69	0.83	0.22	0.06	0.51	0.04				
MgO	21.81	2.62	34.52	1.08	19.47	1.08	34.49	1.48	17.57	1.50	33.97	1.28	0.50	0.20	21.86	3.05	22.10	1.08	41.89	0.51	21.66	1.92	43.18	0.83	20.37	0.66	39.08	0.58	43.79	0.96				
CaO	3.16	0.50	1.30	0.81	2.57	0.29	0.68	0.06	2.58	0.30	0.77	0.33	0.10	0.01	2.19	0.28	2.71	0.29	0.03	0.04	3.34	0.31	0.06	0.06	3.19	0.14	0.00	0.03	0.00	0.00				
Cr <sub>2</sub> O <sub>3</sub>	0.81	0.52	0.24	0.07	1.50	1.11	0.20	0.08	0.47	0.31	0.10	0.02	0.02	0.04	0.30	0.11	0.42	0.05	0.27	0.02	0.44	0.02	0.29	0.05	0.38	0.04	0.20	0.02	0.34	0.03				
MnO	0.29	0.03	0.24	0.07	0.41	0.06	0.33	0.11	0.41	0.09	0.47	0.06	0.03	0.02	0.32	0.02	0.38	0.02	0.17	0.05	0.39	0.13	0.12	0.03	0.45	0.10	0.17	0.04	0.14	0.02				
NiO	0.02	0.02	0.01	0.01	0.00	0.00	0.04	0.02	0.01	0.02	0.07	0.04	0.02	0.03	0.05	0.02	0.00	0.00	0.14	0.12	0.00	0.00	0.00	0.00	0.00	0.00	0.22	0.07	0.28	0.04				
Totals	100.66		100.35		100.86		102.41		100.95		102.11		101.51		97.51		99.91		100.03		99.97		99.79		99.98		99.86		99.94					
Na <sub>2</sub> O/ K <sub>2</sub> O	82.2		4.8		79.6		19.7		56.5		12.5		0.05		102.7		8.2		3.0		11.0		10.2		15.7		69.0		5.2					
Si	3.862		0.966		3.938		0.972		4.000		0.975		3.012		3.903		3.858		1.014		3.769		1.005		3.737		1.022		1.017					
Na	0.551		0.015		0.751		0.026		0.842		0.042		0.068		0.432		0.796		0.033		0.830		0.045		1.006		0.052		0.051					
K	0.011		0.002		0.006		0.001		0.010		0.002		0.911		0.000		0.068		0.007		0.050		0.003		0.041		0.001		0.006					
Ti	0.000		0.003		0.002		0.003		0.000		0.003		0.000		0.000		0.003		0.001		0.004		0.000		0.008		0.000		0.000					
Fe	0.323		0.086		0.361		0.121		0.405		0.117		0.028		0.472		0.394		0.338		0.457		0.311		0.395		0.411		0.267					
Al	0.743		0.036		0.683		0.008		0.708		0.006		0.947		0.653		0.589		0.012		0.654		0.012		0.780		0.006		0.015					
Mg	2.245		0.886		2.016		0.880		1.818		0.871		0.031		2.344		2.292		1.578		2.268		1.621		2.117		1.497		1.629					
Ca	0.234		0.023		0.191		0.013		0.188		0.014		0.000		0.169		0.200		0.001		0.247		0.001		0.237		0.000		0.000					
Cr	0.047		0.006		0.082		0.003		0.021		0.001		0.000		0.021		0.023		0.005		0.025		0.006		0.016		0.003		0.006					
Mn	0.021		0.003		0.024		0.005		0.018		0.006		0.000		0.023		0.022		0.004		0.020		0.003		0.024		0.003		0.003					
Ni	0.000		0.000		0.000		0.001		0.000		0.000		0.000		0.005		0.000		0.003		0.000		0.000		0.000		0.004		0.006					
Totals	8.037		2.026		8.055		2.033		8.010		2.037		4.997		8.022		8.245		2.996		8.324		3.007		8.361		2.999		3.000					
Oxygens	12		3		12		3		12		3		8		12		12		4		12		4		12		4		4					

Gt: garnet; Pv: (Mg,Fe)SiO<sub>3</sub> perovskite; Rgt: ringwoodite; Wds: wadsleyite; Hlt: hollandite. Numbers in parentheses: analysis number; S.D.: standard deviations of analyses.

Table 4. Compositions of magnesiowüstite (Mw) in wt.%.

	H 2366		H 2237		H 2236		H 2368	
	Mw (5)	STDEV	Mw (5)	STDEV	Mw (5)	STDEV	Mw (5)	STDEV
SiO <sub>2</sub>	0.50	0.16	0.56	0.11	0.39	0.16	0.59	0.19
Na <sub>2</sub> O	3.30	0.66	2.16	1.06	1.88	0.15	1.83	0.22
K <sub>2</sub> O	0.05	0.03	0.05	0.09	0.02	0.01	0.03	0.02
TiO <sub>2</sub>	0.06	0.05	0.08	0.08	0.02	0.01	0.03	0.06
FeO	49.56	11.43	38.86	5.28	38.63	1.77	38.65	5.56
Al <sub>2</sub> O <sub>3</sub>	1.27	0.48	0.41	0.12	0.59	0.05	0.35	0.07
MgO	43.52	12.37	57.17	6.12	58.08	1.89	54.29	6.85
CaO	0.11	0.03	0.06	0.04	0.06	0.01	0.04	0.01
Cr <sub>2</sub> O <sub>3</sub>	1.67	0.37	1.99	2.22	1.68	0.05	0.95	0.17
MnO	0.62	0.14	0.59	0.20	0.47	0.07	0.58	0.03
NiO	1.29	0.34	0.43	0.59	0.88	0.12	0.21	0.06
Totals	101.95		102.36		102.70		97.55	
Na <sub>2</sub> O/K <sub>2</sub> O	66		43		94		61	
Si	0.004		0.005		0.003		0.005	
Na	0.056		0.033		0.029		0.029	
K	0.000		0.000		0.000		0.000	
Ti	0.000		0.000		0.000		0.000	
Fe	0.365		0.243		0.257		0.272	
Al	0.013		0.004		0.006		0.003	
Mg	0.546		0.680		0.688		0.682	
Ca	0.001		0.001		0.000		0.000	
Cr	0.011		0.013		0.011		0.006	
Mn	0.005		0.004		0.003		0.004	
Ni	0.009		0.003		0.006		0.001	
Totals	1.010		0.986		1.003		1.002	
Oxygens	1		1		1		1	

Numbers in parentheses are analysis number.

ments was sufficient to establish equilibrium. In comparison to the melting experiments of Wang & Takahashi (1999), Agee (1990) and Agee *et al.* (1995), melting durations of 2–10 minutes above the solidus revealed that melting was complete within this time. Melting P–T conditions were deduced from the phase diagram of the Allende meteorite (Agee *et al.*, 1995). Quenching was achieved by shutting off the electrical power, followed by a 15 hours decompression. Run products were cast in epoxy, sectioned and polished.

The recovered samples were characterized by reflected light microscopy, field emission scanning electron microscopy in back scattered electron mode, electron microprobe, laser microRaman spectroscopy and X-ray diffraction. Table 2 lists the phase assemblages identified from recovered samples, which were melted at 16, 18, 20, 21, 23, 24, and 25 GPa, respectively.

Special care was taken during the chemical analysis of the individual phases in the high-pressure runs. Compositions of phases were determined using a JXA-8900RL electron microprobe with wavelength dispersive spectrometers and selection of appropriate standards specifically to obtain reliable Na concentrations. Quantitative analyses of silicates and oxides were conducted at 15 kV accelerating voltage and 10 nA sample current, 10 s counting times. The used standards are diopside for Ca and Si, olivine for Mg, fayalite for Fe, jadeite for Na, K-feldspar for K, chromite for Cr, rutile for Ti, and metallic nickel for Ni. We refrained from using albite or albite glass as a standard for Na due to the con-

siderable loss of Na within seconds, regardless if a defocused or focused electron beam was used. This behavior leads to unrealistic elevated concentrations of Na in the individual high-pressure phases under investigation and consequently to false partition coefficients. Our analytical experience indicated that jadeite is one of the best microprobe standards for Na due to the very low and slow Na loss under the electron beam. The standard deviations ( $1\sigma$ ) for the electron microprobe measurements are shown in Tables 3 and 4 and for all analysed phases.

Raman spectroscopic investigations were conducted at the electron probe analysis points before and after the microprobe analysis. Raman spectra were recorded with a Dilor XY spectrometer equipped with confocal optics and a nitrogen-cooled device (CCD) at Ecole Normale Supérieure de Lyon, France. A microscope was used to focus the excitation laser beam (514 nm line, Ar<sup>+</sup> laser) to a 2  $\mu$ m spot and to collect the Raman signal in the backscattered direction. Accumulations are from 120 to 150 seconds. The laser power was 5 to 10 mW.

### 3. Results

In charge H 2548 from 16 GPa, the phase assemblage consists of majorite garnet, ringwoodite and wadsleyite. In charges H 2549 from 18 GPa and H 2547 from 20 GPa, both phase assemblages are garnet plus ringwoodite. In charge H

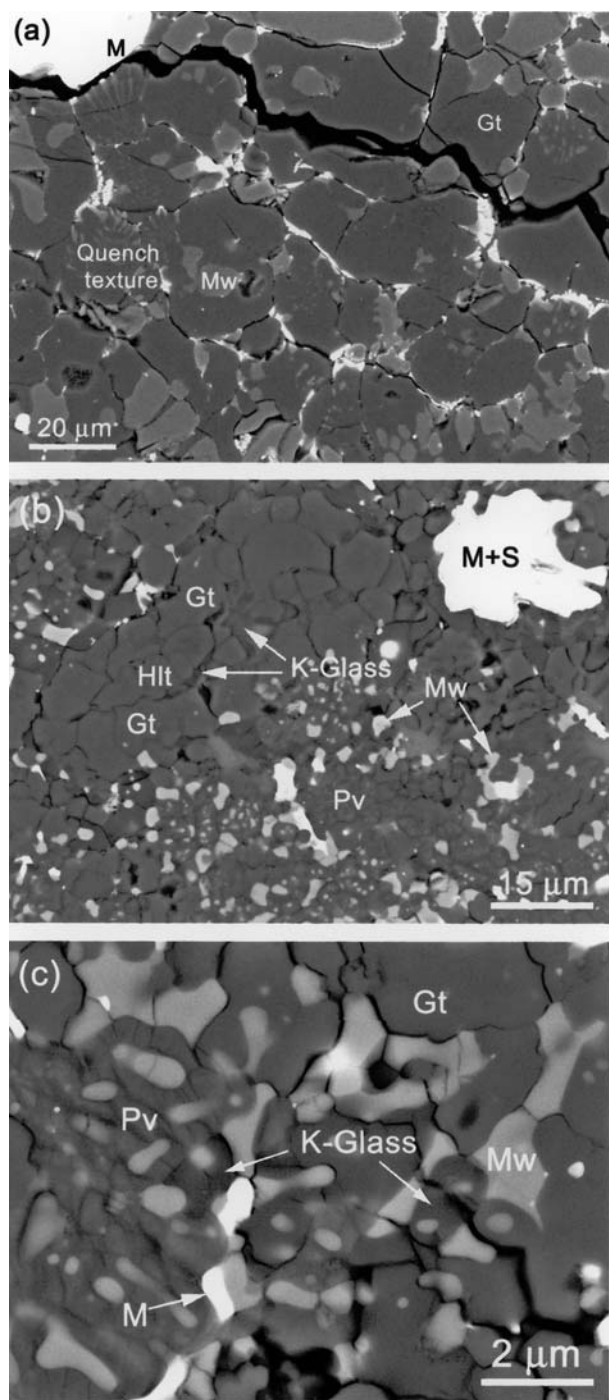


Fig. 2. Back-scattered electron images of polished sections of the run products. Crystalline phases are labeled as Gt (majorite garnet), Pv ( $(\text{Mg,Fe})\text{SiO}_3$  perovskite), Mw (magnesiowüstite), Hlt ( $\text{KAlSi}_3\text{O}_8$  hollandite), K-Glass (K-rich silicate glass), M (metal) and M+S (Fe-Ni-metal plus FeS-sulfide). (a) Quench texture consisting of mottled patches of magnesiowüstite and garnet in the run product of H 2236, 23 GPa, 2000 °C. (b) The high-pressure phase assemblage consisting of garnet, perovskite, magnesiowüstite and small amount of hollandite in the run product of H 2236. A grain of hollandite is surrounded by garnet and K-rich silicate glass in the interstices. (c) K-rich silicate glasses occurring in the interstices of high-pressure phases. Some small grains of magnesiowüstite are enclosed in the K-rich glasses in the run product of H 2237, 24 GPa, 2100 °C.

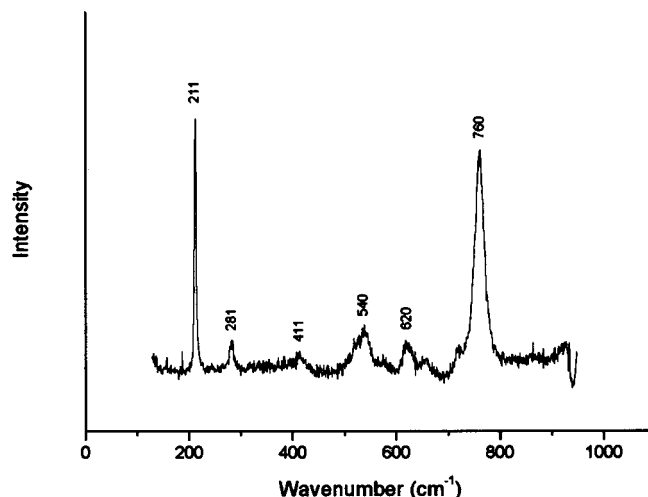


Fig. 3. Raman spectrum of  $\text{KAlSi}_3\text{O}_8$ -hollandite depicts only the characteristic bands at 211, 281, 411, 540, 620 and 760  $\text{cm}^{-1}$ .

2368 from 21 GPa, the phase assemblage is garnet plus magnesiowüstite. In charge H 2236 from 23 GPa, the phase assemblage consists of garnet,  $(\text{Mg,Fe})\text{SiO}_3$ -perovskite, magnesiowüstite and a small amount of  $\text{KAlSi}_3\text{O}_8$ -hollandite. In charges H 2237 from 24 GPa and H 2366 from 25 GPa, high-pressure phases are garnet, perovskite and magnesiowüstite. Evidently, garnet appears in all charges from 16 to 25 GPa. Perovskite first appears above 23 GPa. The abundance of garnet decreases progressively with increasing pressure from 23 to 25 GPa, whereas the abundance of perovskite increases along with pressure increase. At 25 GPa, perovskite becomes the predominant silicate phase in addition to minor amounts of garnet (< 5 % by volume). Magnesiowüstite is also a high-pressure phase at pressures between 21 to 25 GPa, and its abundance increases from 10 to 25 % by volume with increasing pressure. In all experimental runs, immiscible Fe-Ni-S liquid was produced, which quenched as eutectic nodules of FeNi-metal plus FeS sulfide. The  $\text{Na}_2\text{O}$  and  $\text{K}_2\text{O}$  contents of FeNi metal and FeS sulfide are below the detection limits of electron microprobe techniques (< 0.01 wt.%).

Quench textures consisting of mottled patches of magnesiowüstite and garnet were encountered in the run products (Fig. 2a). The presence of the quench textures indicates that melting of the charges have taken place. Such quench textures are identical to those reported by Agee (1990) in the melting experiments of Allende meteorite.

Hollandite-structured  $\text{KAlSi}_3\text{O}_8$  ( $\text{K}_{0.91}\text{Na}_{0.07}\text{AlSi}_3\text{O}_8$ ) was identified in charge H 2236, and its composition and structure was confirmed by electron microprobe analysis, Raman spectroscopy and X-ray diffraction. The grain sizes of hollandite-structured  $\text{KAlSi}_3\text{O}_8$  are up to several micrometers. The grains are usually surrounded by majorite garnet (Fig. 2b). The Raman spectrum of  $\text{KAlSi}_3\text{O}_8$ -hollandite displays only the characteristic bands at 211, 281, 411, 540, 620 and 760  $\text{cm}^{-1}$  (Fig. 3). The intense band at 760  $\text{cm}^{-1}$  corresponds to the Si-O stretching vibration in the  $\text{SiO}_6$  octahedra by comparison with the Raman spectrum of stishovite (Hemley *et al.*, 1986). The Raman bands of  $\text{KAlSi}_3\text{O}_8$ -hol-

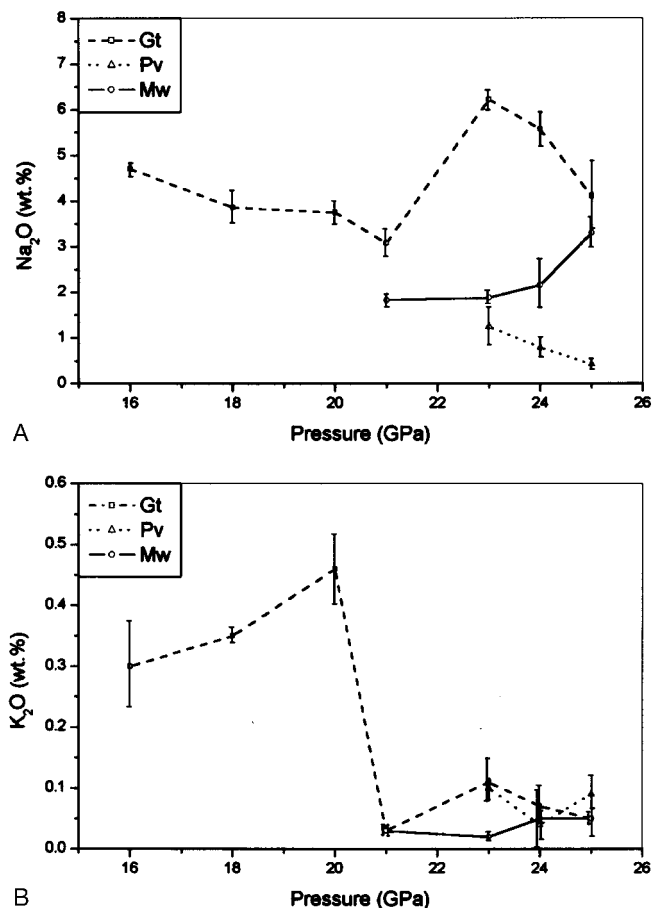


Fig. 4. Variation of Na<sub>2</sub>O and K<sub>2</sub>O contents in garnet (Gt), perovskite (Pv) and magnesiowüstite (Mw) as a function of pressure. The error bars stand for the standard deviation of analyses (one sigma).

landite are similar to those of natural (Na,K)AlSi<sub>3</sub>O<sub>8</sub>-hollandite in the Sixiangkou meteorite and of (Ca,Na)AlSi<sub>3</sub>O<sub>8</sub>-hollandite in the Zagami (SNC) meteorite (Gillet *et al.*, 2000; Chen *et al.*, 2000).

The bulk compositions of experimentally quenched silicate liquids are similar to the bulk composition of starting material (Agee, 1990; Agee *et al.*, 1995). Agee *et al.* (1995) used the compositions of quenched silicate liquids to determine the element partitioning among crystal and liquid. However, the compositional data reported by Agee *et al.* (1995) indicate that the Na<sub>2</sub>O and K<sub>2</sub>O concentrations in the starting material and the quenched silicate liquids at high pressures remain nearly unchanged, for example 0.48 wt.% Na<sub>2</sub>O in the Allende bulk silicate (starting material), 0.41 wt.% Na<sub>2</sub>O in the 10 GPa quench liquid, 0.44 wt.% Na<sub>2</sub>O in the quench liquids of 24 and 26 GPa runs, respectively. Differences should have been found between the concentrations in the quenched silicate liquids, high-pressure phases and starting compositions, if partitioning took place. In fact, we never observe such quench texture similar to experimental run products in the natural samples, *i.e.* the shock veins of chondritic meteorites. In comparison, we found thin silicate glass layers in the interstices between majorite-pyropite garnet solid solution and magnesiowüstite in the shock veins of Sixiangkou meteorite (Chen *et al.*, 1996). Such sili-

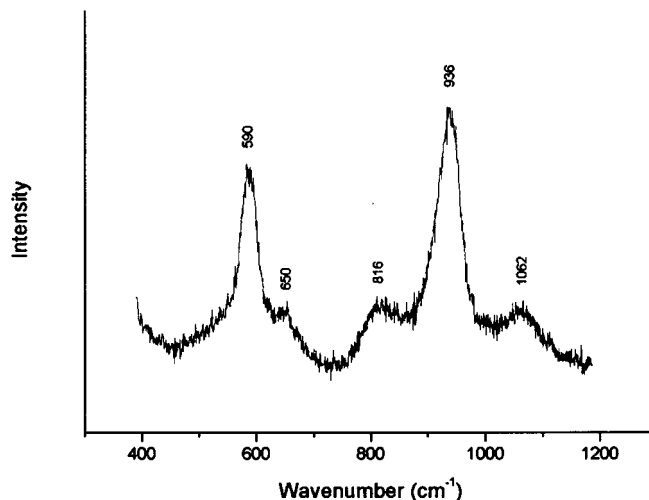


Fig. 5. Raman spectrum of garnet from the charge 23 GPa shows only the characteristic bands of majorite at 590, 650, 816, 936 and 1062 cm<sup>-1</sup>.

cate glass layers could stand for the last quenched melt. For this reason, we tried to search for the silicate melt glass occurring between the dense crystalline phases in the run products, and to investigate the crystal/liquid partition of alkali elements. Less than 2% by volume of melt glass was found in nearly all run products. These glasses occur only as small specks and are usually distributed in the interstices of high-pressure phases or wet their surfaces (Fig. 2b, 2c). The glass is very sensitive to the electron beam irradiation of the microprobe, and it is easily degraded under normal analysis conditions. The sizes of glasses between <1 μm and 2 μm are too small for conducting quantitative EPMA analysis, which inhibited us from quantitatively determining the crystal/liquid partition measurements. The only information we have from semiquantitative EDX analyses in the charges above 21 GPa shows that the compositions of quench melt glasses vary from grain to grain within the range: SiO<sub>2</sub>, 35-50 wt.%; MgO, 20-30 wt.%; FeO, 8-15 wt.%; K<sub>2</sub>O, 7-12 wt.%; Na<sub>2</sub>O, 2-7 wt.%; Na<sub>2</sub>O/K<sub>2</sub>O, 0.16-1. The K-rich nature of these glasses has also been confirmed by K X-ray maps. We suggest that these K-rich glasses could be the quenched melt that was enriched in K, in which the crystal/melt partition coefficient of K<sub>2</sub>O ( $D_{K_2O}$ ), is 0.01-0.005 in garnet, ≤0.01 in perovskite and magnesiowüstite. Potassium only preferentially partitions into KAlSi<sub>3</sub>O<sub>8</sub>-hollandite, and its  $D_{K_2O}$  is ~1.64.

Na<sub>2</sub>O contents in garnet are correlated with pressure and occurrence of other co-existing phases (Table 3-4; Fig. 4). Below 20 GPa, majorite contains 3.75-4.71 wt.% Na<sub>2</sub>O. Presence of Na-bearing magnesiowüstite at 21 GPa results in a decrease of Na<sub>2</sub>O content of garnet (3.08 wt.%). However, appearance of perovskite at 23 GPa results in an increase of Na<sub>2</sub>O content of garnet (6.22 wt.%). At high-pressure above 23 GPa, Na<sub>2</sub>O contents in garnet and perovskite are negatively correlated with pressure, in which Na<sub>2</sub>O contents in garnet decrease from 6.22 wt.% at 23 GPa to 4.11 wt.% at 25 GPa, and Na<sub>2</sub>O contents in perovskite decrease from 1.25 wt.% at 23 GPa to 0.43 wt.% at 25 GPa. Raman

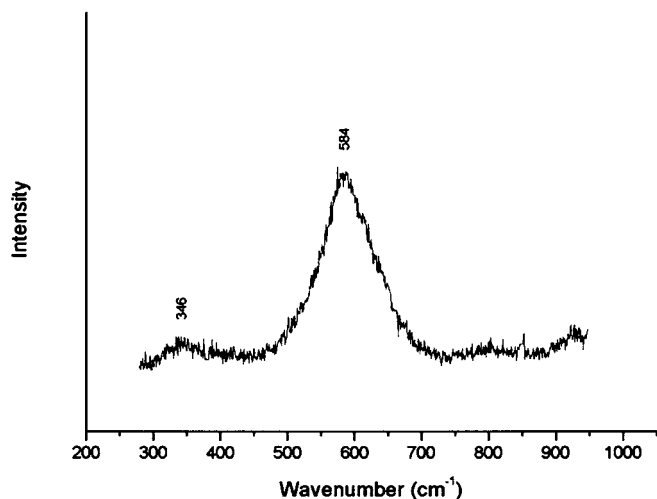


Fig. 6. Raman spectrum of perovskite from the charge 24 GPa shows two broad bands at 346 and 584  $\text{cm}^{-1}$ , which is indicative of amorphous phase. Also here, there are no other bands of other phases.

spectra of the garnet grains conducted at the same spots that were compositionally analyzed by electron microprobe depict only the characteristic vibration bands of garnet (Fig. 5). Raman spectra of perovskite show two broad bands at 346 and 584  $\text{cm}^{-1}$ , which is indicative of amorphous phase as a result of back-transformation from crystalline perovskite to glass after pressure release (Fig. 6). High-resolution back-scattered electron images of microprobe-analyzed garnets and perovskites display no foreign inclusions. It indicates that the higher Na contents in garnet and perovskite are not due to any kind of contamination. In addition,  $\text{Na}_2\text{O}$  contents in magnesiowüstite increase with increasing pressure from 1.8 wt.% at 21 GPa, to 3.3 wt.% at 25 GPa. Magnesiowüstite is Raman inactive and not any Raman peak was identified for magnesiowüstite grains. However, no other Raman band of a crystalline or amorphous component was present in the spectrum.

#### 4. Discussion

In the garnet structure, isolated  $[\text{SiO}_4]$  tetrahedra interconnect with  $[\text{BO}_6]$  octahedra (B:  $\text{Al}^{3+}$ ,  $\text{Fe}^{3+}$ ,  $\text{Cr}^{3+}$ ), which form larger dodecahedral sites (deformed cube with 8 coordinated cations) for the accommodation of larger cations such as  $\text{Mg}^{2+}$ ,  $\text{Fe}^{2+}$ ,  $\text{Ca}^{2+}$ ,  $\text{Na}^+$ , and  $\text{K}^+$ . The garnet obtained in our experiments is evidently a solid solution between majorite, pyrope and less abundant Na-majorite because it contains abundant  $\text{MgO}$  (17.57–22.10 wt.%) and  $\text{Al}_2\text{O}_3$  (7.30–9.69 wt.%). The components of garnet, which include a certain amount of  $\text{Na}_2\text{O}$  and  $\text{K}_2\text{O}$ , show a coupled substitution of  $[\text{Na} \text{ (or) } \text{K}]$  for  $[\text{Mg} \text{ (or) } \text{Ca}]$  (Ringwood & Major, 1971). Although the radii of both  $\text{Na}^+$  ( $V^{\text{IR}}=0.97 \text{ \AA}$ ) and  $\text{K}^+$  ( $V^{\text{IR}}=1.33 \text{ \AA}$ ) are much larger than that of  $\text{Mg}^{2+}$  ( $V^{\text{IR}}=0.66 \text{ \AA}$ ), the relatively larger compressibility of  $\text{Na}^+$  and  $\text{K}^+$  at high pressure may explain this substitution (Harlow, 1997; Wang & Takahashi, 1999). Wang & Takahashi (1999), who used a K-rich basalt (1.31 wt.%  $\text{K}_2\text{O}$ ) as the starting material

in their melting experiments, found that garnet contains very low  $\text{K}_2\text{O}$  (<0.07 wt.%) at pressures less than 22.5 GPa, but that the  $\text{K}_2\text{O}$  content of garnet increased sharply to 0.50 wt.% at 25 GPa and 1.37 wt.% at 27 GPa, respectively. However, in other experiments using K-doped peridotite (0.64 wt.%  $\text{K}_2\text{O}$ ) as a starting material, Wang & Takahashi (2000) reported that all synthesized garnets at pressures from 10–20 GPa also contain low K contents (<0.18 wt.%), and that K is mainly incorporated in three unknown K-rich phases (*i.e.* phase I, phase II, and phase III) (4.93–14.19 wt.%  $\text{K}_2\text{O}$ ) at pressures 15–25.5 GPa. Na in these experiments is mainly incorporated in garnet, magnesiowüstite, and the unknown K-rich phases. These three unknown K-rich phases contain significant amounts of  $\text{Al}_2\text{O}_3$ . Among these K phases, phases II and III contain 15–46 wt.%  $\text{Al}_2\text{O}_3$ , which are much richer in  $\text{Al}_2\text{O}_3$  than accommodated by the pyrope component of garnet in our experiments (7.3–9.6 wt.%  $\text{Al}_2\text{O}_3$ ). The different behavior of K in Wang & Takahashi's experiments (2000) could be related to the bulk composition of the starting material. For example, the  $\text{Al}_2\text{O}_3$  content (4.13 wt.%) in their starting material is much higher than in our study (2.49 wt.%), and the  $\text{SiO}_2$  content (45.21 wt.%) is lower than ours (51.9 wt.%). The bulk composition in Wang & Takahashi's experiments (2000) is also much richer in  $\text{MgO}$  ( $\text{Mg}^{\#}=0.83$ ) and has a lower  $\text{Na}_2\text{O}/\text{K}_2\text{O}$  ratio (0.45) than in our study ( $\text{Mg}^{\#}=0.73$  and  $\text{Na}_2\text{O}/\text{K}_2\text{O}=7$ ), which may affect melting temperature and Na/K fractionation. Abundant Al in the starting material of Wang & Takahashi's experiments presumably plays an important role in the formation of alumino-silicate phases, and the high Al-content in these alumino-silicate phases may favor the coupled substitutions of  $[\text{K} \text{ (and) } \text{Na}] + \text{Si}$  for  $[\text{Mg} + \text{Al}]$ , hence forming the K-rich phases. No K-hollandite was found in Wang & Takahashi's experiments (2000), which could be due to the lower  $\text{SiO}_2$  content in the bulk composition.

Our experimental results indicate that the elemental substitutions of Na and K in the garnet structure are not positively correlated with pressure in our multiphase system. Garnet contains considerable amounts of Na (3.08–6.22 wt.%  $\text{Na}_2\text{O}$ ) from 16 to 23 GPa, but its  $\text{Na}_2\text{O}$  contents decrease from 6.22 wt.% (23 GPa) to 4.11 wt.% (25 GPa). It contains higher  $\text{K}_2\text{O}$  contents (0.30–0.46 wt.%) at pressures below 20 GPa, but its  $\text{K}_2\text{O}$  contents decrease to a lower level (<0.11 wt.%) at pressures above 21 GPa. This may appear in sharp contrast to the results of Wang & Takahashi (2000), if we do not consider the difference in the compositions of starting materials.

Our results revealed that garnet with a high majorite content contains rather high concentrations of  $\text{Na}_2\text{O}$  (3.75–4.71 wt.%) and moderate  $\text{K}_2\text{O}$  (0.3–0.46 wt.%) at pressures from 16 to 20 GPa. In a phase assemblage consisting of majorite garnet,  $(\text{Mg,Fe})\text{SiO}_3$ -perovskite, and magnesiowüstite at pressures between 21 and 25 GPa in the primitive mantle of the Earth, significant amounts of Na would preferentially partition into magnesiowüstite. As pressure increases, garnet will be replaced by perovskite. Magnesiowüstite becomes a major crystalline phase containing Na at pressures close to 25 GPa as perovskite becomes a predominant silicate phase. This result is in agreement with high-pressure experiments on pyrolite at 28 GPa by Irifune (1994), which

indicate that Na partitions more in favor of magnesiowüstite than of the coexisting Mg- or Ca-perovskites.

High-pressure phases including majorite garnet, (Mg,Fe)-SiO<sub>3</sub>-perovskite, and akimotoite containing considerable amounts of Na were reported in the shock-produced chondritic melt veins of L-chondrites (Price *et al.*, 1979; Chen *et al.*, 1996; Sharp *et al.*, 1997; Tomioka & Fujino, 1999). The textural settings of natural NaAlSi<sub>3</sub>O<sub>8</sub>-rich hollandite in the shock-produced melt veins of Sixiangkou meteorite (Gillet *et al.*, 2000) are indicative of crystallization in isolated plagioclase melt pockets with initial plagioclase-like composition and not from the chondritic melt. This result is of importance for our understanding why no NaAlSi<sub>3</sub>O<sub>8</sub>-hollandite is produced in all our run products, in which complete melting at high pressures were achieved. Majorite garnet, magnesiowüstite, and (Mg,Fe)SiO<sub>3</sub>-perovskite are the major Na-bearing phases in our experiments.

In the high-pressure assemblages from 16 to 20 GPa, garnet is hence the only phase possibly to accommodate moderate amounts of K. The coupled substitutions of [K + Si] for [Mg + Al] may take place more *easily* at elevated pressure. Therefore, K contents in garnet increase at pressures from 16 to 20 GPa. At pressures above 21 GPa, garnet, perovskite and magnesiowüstite contain very low concentrations of K<sub>2</sub>O (<0.1 wt.%), whereas Na is mostly accommodated in these phases, which results in the higher Na<sub>2</sub>O/K<sub>2</sub>O ratios in garnet (56-102), magnesiowüstite (43-94), and perovskite (5-20). This indicates that the Na/K fractionation should have taken place between the high-pressure phases and the silicate melt, since most of K is concentrated in the melt above 21 GPa and partially incorporated in KAlSi<sub>3</sub>O<sub>8</sub>-hollandite at 23 GPa.

Our experiments indicate that if the primitive Earth had accreted from chondritic planetesimals and formed a magma ocean (Agee, 1990) and chondritic mantle (Ringwood, 1979), majoritic garnet could be an important phase for accommodation of both Na<sub>2</sub>O and K<sub>2</sub>O at depths corresponding to pressures from 16 to 20 GPa in the chondritic ratio. At pressures above 21 GPa, Na might also be incorporated into garnet and magnesiowüstite. However, K<sub>2</sub>O contents in coexisting magnesiowüstite, garnet, and perovskite are very low (<0.1 wt.%) at pressures from 21 to 25 GPa. Above ~23 GPa, K mainly resides in the melt. These results are in agreement with our previous finding on the Na/K fractionation in naturally shocked L-chondrites at pressures from 20 to 24 GPa. Garnet and magnesiowüstite in the shock veins of Sixiangkou L6-chondrite acquired most of Na from the shock-produced chondritic melt, whereas K evaporated from the chondritic melt was taken by the maskelynite melt in the neighboring region of veins (Chen *et al.*, 1996; El Goresy *et al.*, 1997a, 1997b; Chen & El Goresy, 2000). Our experimental studies show that fractionation between K and Na should take place in a chondritic melt due to the solid/liquid partitioning behavior of K thus favoring the silicate melts at high-pressures above 21 GPa inside the mantle.

## 5. Conclusions

Majorite garnet might contain apparent amounts of both Na<sub>2</sub>O and K<sub>2</sub>O in chondritic material at pressures from 16 to

20 GPa. At pressures between 21 and 25 GPa, garnet and magnesiowüstite are also the major phases containing Na. In this pressure range (Mg,Fe)SiO<sub>3</sub>-perovskite accommodates only a small amount of Na<sub>2</sub>O. In the high-pressure assemblage consisting of garnet, magnesiowüstite and perovskite, the Na<sub>2</sub>O content in magnesiowüstite correlates positively with pressure, whereas the Na<sub>2</sub>O content of majorite garnet and perovskite progressively decreases with increase of pressure. This shows that Na partitions favorably into magnesiowüstite at higher pressure. Our experiments strongly suggest that magnesiowüstite is the major Na-bearing phase in the lower mantle. K is mostly concentrated in the silicate melt above 21 GPa and is partially incorporated in KAlSi<sub>3</sub>O<sub>8</sub>-hollandite at this pressure regime (such as those at 23 GPa). Our melting experiments indicate that Na/K fractionation may have occurred in the chondritic primitive mantle of the Earth at pressures above 21 GPa due to the partitioning behavior of K to the silicate melt.

In comparing our results with other previous data, the contents of Al and Si in the starting material could also play an important role in the formation of K-rich phases. Relatively high Al<sub>2</sub>O<sub>3</sub>-content may be available for the formation of K-rich aluminosilicate phases (phase I, II, III of Wang & Takahashi, 2000), whereas relatively high SiO<sub>2</sub>-content is necessary for the formation of K-hollandite.

**Acknowledgments:** This work was supported by the Deutsche Forschungsgemeinschaft (Grant Go 315/15-1), and the Chinese Academy of Sciences under grant KZCX3-SW-123, KJCX2-SW-NO3 and the Hundred Talents Program. We thank Denis Andrault, Rainer Altherr and Nathalie Bolfan-Casanova for constructive reviews, which lead to considerable improvement of the manuscript.

## References

- Agee, C.B. (1990): A new look at differentiation of the Earth from melting experiments on the Allende meteorite. *Nature*, **346**, 834-837.
- Agee, C.B., Li, J., Shannon, M.C., Circone, S. (1995): Pressure-temperature phase diagram for the Allende meteorite. *J. Geophys. Res.*, **100**, 17725-17740.
- Chen, M. & El Goresy, A. (2000): The nature of maskelynite in shocked meteorites: not diaplectic glass but a glass quenched from shock-induced dense melt at high pressures. *Earth Planet. Sci. Lett.*, **179**, 489-502.
- Chen, M., Sharp, T.G., El Goresy, A., Wopenka, B., Xie, X. (1996): The majorite-pyrope + magnesiowüstite assemblage: constraints on the history of shock veins in chondrites. *Science*, **271**, 1570-1573.
- Chen, M., El Goresy, A., Gillet, P. (2000): Hollandite-type (Ca,Na)AlSi<sub>3</sub>O<sub>8</sub> in a shock vein of Zagami (SNC) meteorite., *Ber. dt. mineral. Ges., Beih. z. Eur. J. Mineral.*, Vol. **12**, No. 1, 30.
- El Goresy, A., Wopenka, B., Chen, M., Weinbruch, S., Sharp, T. (1997a): Evidence for two different shock induced high-pressure events and alkali vapor metasomatism in the Peace River and Tenham (L6) chondrites. 28<sup>th</sup> Lunar and Planetary Sciences Conference.
- El Goresy, A., Wopenka, B., Chen, M., Kurat, G. (1997b): The saga of maskelynite in Shergotty. *Meteoritics*, **32**, A38-39.



- El Goresy, A., Chen, M., Gillet, P., Durovinsky, L. (2000): Shock-induced high-pressure phase transition of labradorite to hollandite ( $\text{Na}_{47}\text{Ca}_{51}\text{K}_2$ ) in Zagami and the assemblage hollandite “( $\text{Na}_{80}\text{Ca}_{12}\text{K}_8$ ) plus jadeite” in L chondrites: Constraints to peak shock pressures. *Meteorit. Planet. Sci.*, **35**, A51.
- Gillet, Ph., Chen, M., Dubrovinsky, L., El Goresy, A. (2000): Natural  $\text{NaAlSi}_3\text{O}_8$ -hollandite in the shocked Sixiangkou meteorite. *Science*, **287**, 1633-1636.
- Harlow, G.E. (1997): K in clinopyroxene at high pressure and temperature: An experimental study. *Am. Mineral.*, **82**, 259-269.
- Hemley, J., Mao, H.K., Chao, E.C.T. (1986): Raman spectrum of natural and synthetic stishovite. *Phys. Chem. Minerals*, **13**, 285-290.
- Herzberg, C. & Zhang, J. (1996): Melting experiments on anhydrous peridotite KLB-1: Compositions of magmas in the upper mantle and transition zone. *J. Geophys. Res.*, **101** (B4), 8271-8295.
- Irfune, T. (1994): Absence of an aluminous phase in the upper part of the Earth's mantle. *Nature*, **370**, 131-133.
- Kallemeyn, G.W. (1988): Elemental variations in bulk chondritis: A brief review. In: Kerridge, J.F. & Matthews, M.S. (Eds.), “Meteorites and Early Solar System”, University of Arizona Press, Tucson, 390-393.
- Langenhorst, F. & Poirier J.P. (2000): ‘Eclogitic’ minerals in a shocked basaltic meteorite. *Earth Planet. Sci. Lett.*, **176**, 259-265.
- Liu, L. (1978): High-pressure phase transformations of albite, jadeite and nepheline. *Earth Planet. Sci. Lett.*, **37**, 438-444.
- Mason, B. (1966): Composition of the Earth. *Nature*, **211**, 616-618.
- Morgan, J.W., Wandless, G.A., Petrie, R.K., Irving, A.J. (1980): Composition of the Earth's upper mantle – II: Volatile trace elements in ultramafic xenoliths. *Proc. Lunar Planet. Sci. Conf. 11th, Geochim. Cosmochim. Acta, Suppl.* **14**, 213-233.
- Price, G.D., Putnis, A., Agrell, S.O. (1979): Electron petrography of shock-produced veins in the Tenham chondrite. *Contrib. Mineral. Petrol.*, **71**, 211-218.
- Ringwood, A.E. (1975): Composition and Petrology of the Earth's Mantle. McGraw-Hill, New York, NY. 544 pp.
- (1979): Origin of the Earth and Moon. Springer-Verlag, New York, NY. 295 pp.
- Ringwood, A.E. & Major, A. (1971): Synthesis of majorite and other high pressure garnets and perovskites. *Earth Planet Sci. Lett.*, **12**, 411-418.
- Sharp, T.G., Lingemann, C.M., Dupas, C., Stöffler, D. (1997): Natural occurrence of  $\text{MgSiO}_3$ -ilmenite and evidence for  $\text{MgSiO}_3$ -perovskite in a shocked L chondrite. *Science*, **277**, 352-355.
- Tomioka, N. & Fujino, K. (1999): Akimotoite,  $(\text{MgFe})\text{SiO}_3$ , a new silicate mineral of the ilmenite group in the Tenham chondrite. *Am. Mineral.*, **84**, 267-271.
- Wang, W. & Takahashi, E. (1999): Subsolidus and melting experiments of a K-rich basaltic composition to 27 GPa: Implication for the behavior of potassium in the mantle. *Am. Mineral.*, **84**, 357-361.
- , – (2000): Subsolidus and melting experiments of K-doped peridotite KLB-1 to 27 GPa: Its geophysical and geochemical implications. *J. Geophys. Res.*, **105**, 2855-2868.
- Yagi, A., Suzuki, T., Akaogi, M. (1994): High pressure transitions in the system  $\text{KAlSi}_3\text{O}_8$ - $\text{NaAlSi}_3\text{O}_8$ . *Phys. Chem. Minerals*, **21**, 12-17.

Received 22 February 2003

Modified version received 11 September 2003

Accepted 16 October 2003

